

Make Your Actor Talk: Generalizable and High-Fidelity Lip Sync with Motion and Appearance Disentanglement

Runyi Yu¹, Tianyu He, Ailing Zhang¹, Yuchi Wang¹, Junliang Guo, Xu Tan, Chang Liu³, Jie Chen^{1,2}, and Jiang Bian

¹Peking University ²Peng Cheng Laboratory ³Tsinghua University

ingrid_yu@stu.pku.edu.cn

<https://Ingrid789.github.io/MyTalk/>



Fig. 1: Samples of the original talking videos and the ones generated by our method according to the given speech input, showcasing that our method performs well in both lip sync and visual detail preservation. It also generalizes well to the unknown and out-of-domain characters (e.g., the bottom case), enabling seamless lip sync for AI-generated videos (e.g., the middle and bottom cases).

Abstract. We aim to edit the lip movements in talking video according to the given speech while preserving the personal identity and visual details. The task can be decomposed into two sub-problems: (1) speech-driven lip motion generation and (2) visual appearance synthesis. Current solutions handle the two sub-problems within a single generative model, resulting in a challenging trade-off between lip-sync quality and visual details preservation. Instead, we propose to disentangle the motion and appearance, and then generate them one by one with a speech-to-motion diffusion model and a motion-conditioned appearance generation model. However, there still remain challenges in each stage, such as motion-aware identity preservation in (1) and visual details preservation in (2). Therefore, to preserve personal identity, we adopt landmarks to represent the motion, and further employ a landmark-based identity loss. To capture motion-agnostic visual details, we use separate encoders to encode the lip, non-lip appearance and motion, and then integrate them with a learned fusion module. We train MyTalk on a large-scale and diverse dataset. Experiments show that our method generalizes well to the unknown, even out-of-domain person, in terms of both lip sync and visual detail preservation. We encourage the readers to watch the videos on our project page.

Keywords: Talking Video Generation · Lip Sync · Facial Animation · Diffusion Model

1 Introduction

Given a video that includes talking individuals, speech-driven talking video lip sync re-generates the lip motion in line with the speech content while preserving the personal identity and appearance visual details [27, 34]. It has huge application prospects in industries like education, live streaming, etc. Recently, with the significant advancements made in AI-generated videos [2, 3, 16, 24], it also shows great potential in editing the lip motion of the generated actors as shown in Fig. 1.

Due to the significant domain gap between visual and speech content, generating visual content that adheres to the visual identity and speech content at the same time is difficult. Early attempts train or adapt a specific model for each person [10, 15, 33, 34], where the identity information is implicitly memorized in the model weights. Although high-quality synthesis is achieved, the trained model can not be employed for unknown persons, thus limiting its broader application. Several studies tackle this challenge by learning the identity and facial appearance in an in-content manner [6, 13, 27, 32, 35]. For example, Wav2Lip [27] masks the lower-half face of the input video and generates the masked region conditioned on the input speech and the reference frames. By training on abundant identities, the model learns to infer the masked facial appearance from the given reference frames. Along this line, the following works further improve the diversity, lip movements and visual quality [6, 13, 32, 35], etc. However, the methods

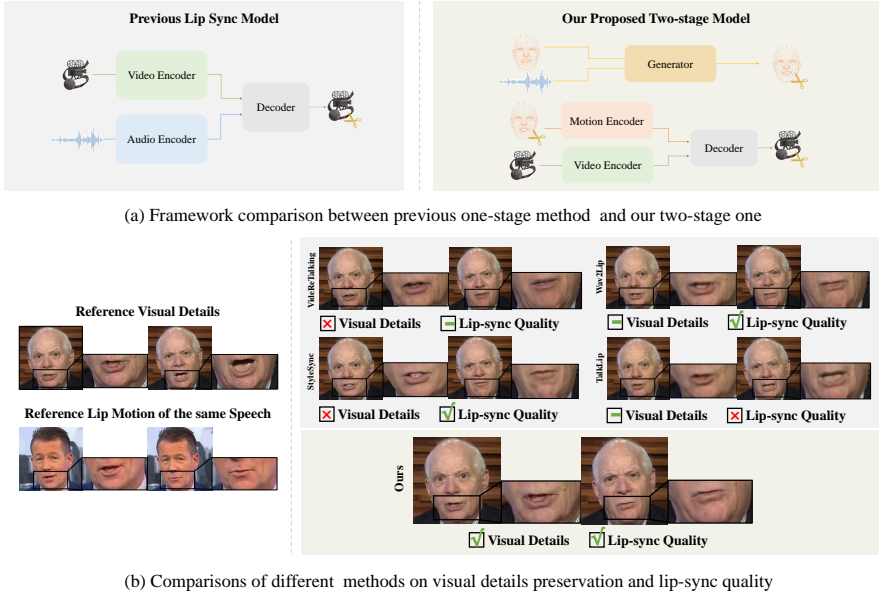


Fig. 2: A brief illustration of previous methods and ours. We compare the edited talking videos generated by different models to evaluate their visual details preservation and lip-sync quality. (a) gives a straightforward framework comparison. (b) shows the evaluation of different methods of visual detail preservation and lip-sync quality. Previous one-stage methods all struggle to simultaneously preserve visual details and ensure lip-sync quality, while our proposed motion-appearance disentangled two-stage method achieves excellent results in both aspects.

above all follow a one-stage framework: the speech-driven lip motion generation and identity-aware appearance generation are handled within a single model, and the vision-speech alignment difficulty makes these methods a trade-off between lip-sync quality and visual details. Fig 2 gives the visual illustration.

In this work, we observe that the motion depicted by landmarks [42] can serve as a mediator reducing the disparity between the visual and speech domains. Accordingly, we propose to disentangle the motion and appearance in talking video, and generate them one by one in a two-stage framework. This insight is also inspired by previous work on talking video generation with a single portrait image [18], however, there still remain challenges for each stage: First, it is crucial to preserve the personal identity during the motion generation, such as ensuring consistency of face contours between the original and the generated one. Second, it is non-trivial to generate person-specific details in the lip region while preserving the dynamic non-lip region in the original video. To realize appearance and motion disentanglement and overcome the challenges, we present **Make Your Actor Talk**, abbreviated as **MyTalk**. It consists of two models: a speech-to-motion diffusion model that generates facial landmarks [42] according

to the input speech, and a motion-conditioned appearance generation model that synthesizes the output video conditioned on the generated landmarks and reference frames. To tackle the above two challenges, for the speech-to-motion diffusion model, we introduce the extracted identity feature as an extra condition and employ a landmark-based identity loss to preserve personal identity. For the motion-conditioned appearance generation model, since the reference frames are with different motions, to capture motion-agnostic visual details, we use three encoders: a lip appearance encoder, a non-lip appearance encoder, and a landmark encoder to encode the appearance and motion representations. The learned representations are fused and then decoded to output videos using the decoder.

To enable better generalization, we train MyTalk on a large-scale and diverse dataset that consists of 15K unique identities. Experimental results demonstrate that MyTalk achieves excellent results in visual detail preservation and lip-sync quality. Owing to the superiority of the disentangled modeling, it also generalizes well to the unknown characters in unseen domains (see Fig. 1), and enables interesting appearance editing and emotion control on the original video as shown in Fig. 4. To conclude, our contributions can be summarized as:

- We leverage motion (i.e., landmarks) to reduce the disparity between the video and speech content domains, and further model the talking video lip sync into two sub-problems: speech-driven motion generation and motion-conditioned visual appearance synthesis.
- We propose MyTalk, a new two-stage lip sync method, which disentangles the motion and appearance and generates them step-by-step with separate models.
- To preserve personal identity, we introduce the extracted identity feature as an extra condition and employ a landmark-based identity loss. To capture motion-agnostic visual details, we use separate encoders to encode the motion, lip and non-lip appearance, and combine them with a learnable fusion module.
- With the scaled training data, MyTalk generalizes well to the unknown and out-of-domain characters, it also shows great controllability in terms of lip appearance and talking emotions.

2 Related Work

Talking video generation aims to generate talking videos with lip movements synchronized with the given speech [6, 13, 15, 18, 27, 33, 44]. There are two main subdivisions in this field, including talking video generation and lip sync.

2.1 Speech-driven Talking Video Generation

Talking video generation aims to generate lifelike talking videos according to a speech and single portrait reference image. This requires the model to generate

consistent identity, natural head pose and high-quality lip motion. Various works leverage structural information as the intermediate representation such as landmarks [5, 18, 39, 47], 3D Morphable Models [1, 28, 44, 45] and 3D meshes [4]. Since structural information is still coupled with complex information, these methods typically require additional processing to ensure effective generation, such as MakeItTalk [47] decompose the content and speaker information from the speech; PC-AVS [46] and GAIA [18] disentangles the head pose and facial expression. Recently, NeRF [15, 31] is also introduced in talking video generation, which requires person-specific training and performs poorly across identity.

In this work, we take inspiration from GAIA [18] to leverage structural information and introduce it into the talking video lip sync. We also propose novel techniques to handle personal identity and visual detail preservation.

2.2 Speech-driven Talking Video Lip Sync

Speech-driven talking video lip sync aims to generate the edited talking video with lip movements re-synchronized to the speech and others, e.g. head motion, identity appearance and background dynamics, remaining identical to the given video. The challenges mainly focus on visual detail preservation and lip sync. Some works [15, 34, 41] train or fine-tune a specific model for each identity, which achieves impressive results in identity visual details and lip-sync quality. However, the specific trained models cannot generalize across different identities. Other methods adopt an end-to-end framework and show great robustness in personal identity. Before the diffusion emerges, GANs [8, 12, 27] are usually used as the primary techniques. LipGAN [25] is the first commonly known GAN-based method, and Wav2Lip [27] boosts the lip-sync quality by introducing a pre-trained discriminator. Similarly, the latter work [35] adopts a lip-reading expert to further elevate lip sync. VideoReTalking [6] incorporates several pre-processing and post-processing that significantly enhance the visual quality, and StyleSync [13] strengthens the personalized generation. A recent work DiffTalk [32] tries to edit the talking video in latent space, and models the generation in a diffusion way.

We note that all these generalized methods handle lip motion and appearance generation within a single model. However, as visualized in Fig. 2, these one-stage models struggle to simultaneously process the visual and speech content, resulting in a trade-off between visual details preservation and lip-sync quality.

3 Method

3.1 Preliminary

Problem Definition. Given a talking video x and a speech sequence s , talking video lip sync aims to generate video \hat{x} that lip synchronized with speech s and the dynamic non-lip regions adhere to the original video x .

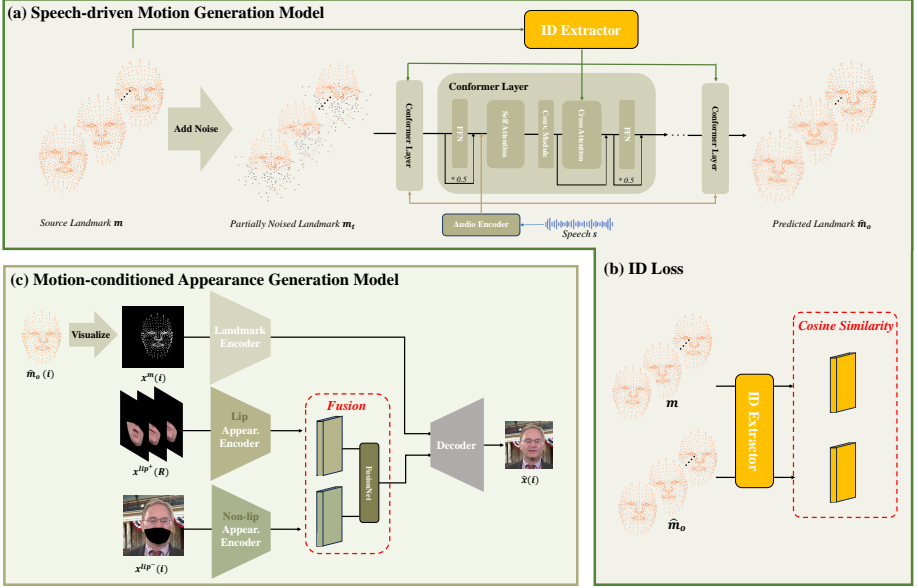


Fig. 3: Our proposed MyTalk adopts a motion-appearance disentangled two-stage framework to realize talking video lip sync. (a) In the first stage, we adopt a speech-driven motion generation model to generate motion (i.e., landmark) sequences from the input speech with the diffusion model. (b) To better preserve the motion identity, we design an identity extractor and the corresponding identity loss in the motion generation model. (c) In the second stage, we use separate encoders to encode the motion-agnostic lip, non-lip appearance, and the generated motion. The encoded representations are fused with a FusionNet and decoded to the output video.

Previous Solutions. Previous works typically use a one-stage model to edit the lip movements in talking videos, as shown in the right part in Fig. 2 (a). These methods can be formulated as:

$$\hat{x} = \mathcal{D}(\mathcal{E}_X(x), \mathcal{E}_S(s)), \quad (1)$$

where \mathcal{E}_X and \mathcal{E}_S represent the video and speech encoder, and \mathcal{D} represents the decoder. Owing to the significant domain gap between visual x and speech s signals, these one-stage models struggle to align the vision and speech features, resulting in the loss of visual details or inferior lip-sync quality.

3.2 Overview

To reduce the disparity between the visual and speech content, we propose MyTalk which decomposes the talking video lip sync into two stages as shown in Fig 3. In the first stage, we adopt dense landmarks [42] as the motion representation and present a speech-driven motion generation model that generates

landmarks according to the input speech. The generated landmarks are then represented as 2D images and leveraged in the second stage. To preserve personal identity, we introduce the extracted identity features as an extra condition and employ a landmark-based identity loss. In the second stage, we propose a motion-conditioned appearance generation model that synthesizes the video according to the landmark images and reference frames. Since our goal is to generate the lip region while preserving the dynamic non-lip region, we encode lip, non-lip appearance and motion with three separate encoders. The encoded features are then fused with a FusionNet followed by a decoder to produce output video.

3.3 Speech-driven Motion Generation

Given the input speech, the speech-driven motion generation model is expected to predict the aligned motion corresponding to the speech content. To achieve this, we use the dense landmark [42] as the motion representation and extract the landmarks m from the given talking video as the input information. For the input speech, we extract its feature using a pre-trained wav2vec model [30]. After obtaining the original landmarks and speech feature, we employ a diffusion model [20, 37, 38] with Conformer backbone [14] to generate the motion sequence conditioned on the speech feature and identity information extracted from reference landmarks. It should be noted that, since our goal is to re-generate the lip motion while preserving the dynamics of the non-lip regions, we also make the generation conditioned on the landmarks of the upper face m^{nl} and only yield the landmarks of the lower face m^l .

Diffusion Model. In the forward diffusion process, the landmarks of the lower face m^l undergo a progressive noising process, making it into Gaussian noise over an infinite number of time steps. The noising process can be formulated as:

$$q(m_t^l | m_{t-1}^l) = \mathcal{N}(\sqrt{\alpha_t} m_{t-1}^l, (1 - \alpha_t)I), \quad (2)$$

where $\alpha_t \in (0, 1)$ is a constant hyper-parameter, and m_0^l is drawn from the data distribution. When α_t is small enough, we can approximate $m_t^l \sim \mathcal{N}(0, I)$.

Subsequently, in the reverse diffusion phase, the model learns the distribution $p(m_0^l | C)$ and reconstructs the original landmark \hat{m}_0^l by denoising the m_t^l . In practice, to ensure the smoothness between the upper face and the generated lower face, we add the landmarks of the upper face m^{nl} of the current frame as the prefix of Conformer input. Therefore, each reverse diffusion step can be formulated as:

$$\hat{m}_0^l = \mathcal{G}(m_t^l | C, m^{nl}), \quad (3)$$

where \mathcal{G} represents the Conformer backbone, and C represents the conditions (i.e., the speech feature, the diffusion time step and identity embedding extracted from reference landmarks). We concatenate the generated landmarks of the lower face \hat{m}_0^l with the given landmarks of the upper face m^{nl} to formulate the motion output \hat{m}_0 .

Identity Preservation. Since the landmarks express facial contours that convey identity information in the form of facial shapes. Owing to the lack of identity constraint, the motion generation model may struggle to produce identity-aware landmark sequences solely with the reconstruction loss. The insight here is that the reconstruction objective is a low-level constraint for landmarks, while identity preservation is a high-level target, which calls for a corresponding high-level constraint. To this end, we first train a facial recognition model (i.e., the identity extractor \mathcal{M}) that takes the facial landmarks as input and outputs the facial embeddings. This model is composed of several MLP layers and trained with the ArcFace [9] loss, which facilitates the embeddings that belong to the same person to be close. Then, we integrate the pre-trained identity extractor into the motion generation model in two ways: (1) We regard the embeddings extracted from the reference landmarks as the condition during the generation. (2) We employ an identity loss that minimizes the embeddings extracted from the reference landmarks and the generation landmarks.

Conditioning. Our conditions C consist of the speech feature z^s , the noise time step t , and the identity embedding z^{id} . To give the conditions to the diffusion model, for noise time step t , we project it into a sinusoidal encoding and further add it to the input of each Conformer layer. For speech z^s and identity z^{id} feature, we first project them into the Conformer dimensions with MLP. Subsequently, we add the projected z^s to the hidden feature of each Conformer block in an element-wise manner and integrate the projected z^{id} into the Conformer block via cross-attention.

Training. We expect our diffusion model to reconstruct the motion sequence under the speech condition and simultaneously ensure consistency of personal identity. Hence, the denoising process can be optimized with the following objective:

$$L_{DM} = \mathbb{E}_{m,C} \left[\|\hat{m}_0 - m\|_2^2 \right] + \mathbb{E} \left[\|1 - \hat{z}^{id} \cdot z^{idT}\| \right], \quad (4)$$

where $C = \{t, z^s, z^{id}\}$ represents the conditions. \hat{z}^{id} and z^{id} are the identity embedding obtained with identity extractor \mathcal{M} .

3.4 Motion-conditioned Appearance Generation

Given the generated landmarks \hat{m} from the motion generation model, the appearance generation model is responsible for producing the output video conditioned on the generated landmarks and reference frames. Ideally, it should preserve the visual details of the reference frames and generate talking videos that are synchronized with the landmarks \hat{m} . To this end, we first represent the landmarks in an image way by projecting the coordinates of landmarks to the image coordinate and obtain x^m . After that, inspired by GAIA [18], we leverage a Variational

AutoEncoder (VAE) [23] to synthesize the appearance. However, different from GAIA which generates talking video with a single frame, our goal is to generate the lip region while preserving the dynamic non-lip region. Therefore, we encode the lip region and non-lip region separately, where the non-lip region comes from the given video and the lip region should be generated according to the generated landmarks. Specifically, we employ three encoders: a lip appearance encoder \mathcal{E}_R , a non-lip appearance encoder \mathcal{E}_A and landmark encoder \mathcal{E}_M . The encoded lip and non-lip appearance features are then fused with a FusionNet \mathcal{F} . Finally, the decoder \mathcal{D} takes all features and produces the output video.

Appearance and Motion Encoding. We denote a single video frame as $x(i)$, and its corresponding projected landmark image as $x^m(i)$. With $m(i)$, we can identify the lip and non-lip regions, which enables us to produce lip and non-lip region masked video frame, denoted as $x^l(i)$ and $x^{nl}(i)$, respectively.

To mitigate the risk of missing lip-related details in a single-frame reference, such as occluded teeth information in lip closed frame, we propose a multi-frame reference strategy. Specifically, we randomly select three frames from the same video clip as reference images and get the non-lip region masked out, denoted as $x^l(R)$. For the current frame $x(i)$, we use three encoders to obtain the corresponding features:

$$\begin{aligned} z^l(R) &= \mathcal{E}_R(x^l(R)), \\ z^{nl}(i) &= \mathcal{E}_A(x^{nl}(i)), \\ z^m(i) &= \mathcal{E}_M(x^m(i)), \end{aligned} \tag{5}$$

where $z^l(R)$, $z^{nl}(i)$ and $z^m(i)$ are the encoded features. We use similar model architecture for \mathcal{E}_R , \mathcal{E}_A and \mathcal{E}_M , which is demonstrated in detail in the Appendix.

FusionNet. Since $z^l(R)$ and $z^{nl}(i)$ both represent appearance information, we propose to use FusionNet to integrate them into one feature that contains both lip and non-lip appearance:

$$z^a(i) = \mathcal{F}(z^l(R), z^{nl}(i)), \tag{6}$$

where $z^a(i)$ represents the fused appearance feature. FusionNet \mathcal{F} adopts convolutions to fuse the appearance latent, and its detailed architecture is depicted in the Appendix.

Decoding. We utilize a decoder \mathcal{D} to recover the visual details from appearance latent $z^a(i)$ and lip movements from motion latent $z^m(i)$. These latent features are concatenated together in channel dimension and used for decoding:

$$\hat{x}(i) = \mathcal{D}(z^a(i), z^m(i)). \tag{7}$$

Training. Our appearance generation model is trained with the L1 reconstruction loss. Since the model handles a generative task, we incorporate a VAE training objective with a KL-penalty on the latent. Building on prior studies [11, 18, 29], we incorporate a discriminator loss to further improve the generation visual quality. Specifically, the discriminator \mathcal{D}_{disc} takes the real frame $x(i)$ and reconstructed frame $\hat{x}(i)$ as the input and computes the discriminator loss L_D :

$$L_{disc}(x(i), \hat{x}(i)) = \log \mathcal{D}_{disc}(x(i)) + \log(1 - \mathcal{D}_{disc}(\hat{x}(i))). \quad (8)$$

Adding the reconstruction loss L_{rec} and KL-penalty L_{KL} , we can get our final loss function as:

$$L_{VAE} = \min_P \max_{\mathcal{D}_{disc}} (L_{rec}(x; P) + L_{KL}(x; P) + L_{disc}(x; \mathcal{D}_{disc})), \quad (9)$$

where P denotes the set of parameters within $\mathcal{E}_R, \mathcal{E}_A, \mathcal{E}_M, \mathcal{F}$, and \mathcal{D} .

3.5 Inference

Our method incorporates two models: a speech-driven diffusion model to generate motion and a motion-conditioned appearance generation model to generate the edited talking video. During inference, we obtain the reference motion landmark m from the source video x . Then for the lower face, we start from Gaussian noise and infer the motion sequence \hat{m} conditioned on the input speech, the identity embedding and the obtained landmarks of the upper face with the denosing process [20]. Subsequently, the generated motion sequence \hat{m} , the lip-masked source video x^{nl} and the reference frames $x^l(R)$ are fed together into the appearance generation model to generate the final talking video \hat{x} .

4 Experiments

Comprehensive experiments are conducted to evaluate our proposed MyTalk. We organize the experiments into three parts. Firstly, in Sec. 4.1, we conduct primary experiments to evaluate the generation quality of different models with both objective and subjective assessments. To better measure the lip-sync quality, we conduct additional experiments on generation with random speech input, which evaluates the generated lip-sync quality conditioned on unaligned video-speech pairs. Subsequently, we compare our appearance generation model with the state-of-the-art one. Finally, we conduct elaborate ablation studies on both our motion and appearance generation model, which is demonstrated in Sec. 4.2.

4.1 Experimental Settings

Dataset. Our training data comes from public datasets, including HDTF [45] and CC v1 & v2 [17, 26], and internal collected datasets. Our dataset varies from gender, race, age, and language. The whole dataset includes 16K unique identities and has a cumulative duration of 1.1K hours. All the videos in the dataset

Table 1: Objective comparisons of our model with previous lip sync baselines. MyTalk achieves superior results in visual and lip-sync quality. The state-of-the-art results on visual quality and ID similarity metrics showcase our superiority in preserving visual details.

Method	Objective Evaluation						
	PSNR \uparrow	SSIM \uparrow	LPIPS \downarrow	FID \downarrow	Sync $_{dist}$ \downarrow	Sync $_{conf}$ \uparrow	ID $_{sim}$ \uparrow
Wav2Lip [27]	30.967	0.894	<u>0.095</u>	7.703	6.249	7.829	0.921
VideoReTalking [6]	29.628	0.885	0.101	9.628	6.978	6.986	0.895
TalkLip [35]	<u>31.140</u>	<u>0.896</u>	<u>0.095</u>	<u>7.401</u>	8.107	5.300	<u>0.926</u>
MyTalk (ours)	33.547	0.906	0.091	5.142	<u>6.544</u>	<u>7.461</u>	0.947

Table 2: Objective comparisons on Table 3: Subjective comparisons. The **unpaired test set**. As shown here, metrics reported here specifically refer to: our method has superior and consistent visual quality, lip-sync quality, visual details preservation and identity consistency.

Method	Objective Evaluation		Method	Subjective Evaluation			
	Sync $_{dist}$ \downarrow	ID $_{sim}$ \uparrow		Vis. \uparrow	Sync \uparrow	Detail \uparrow	Consis. \uparrow
Wav2Lip [27]	<u>6.711</u>	0.916	Wav2Lip [27]	3.04	3.32	2.98	3.74
VideoReTalking [6]	7.580	0.694	VideoReTalking [6]	3.83	3.42	3.55	3.78
TalkLip [35]	9.321	<u>0.922</u>	TalkLip [35]	3.35	3.46	3.40	3.90
MyTalk (ours)	6.703	0.943	MyTalk (ours)	4.22	3.94	4.30	4.45

are cropped and processed by following previous work [18] with a 256×256 resolution. We randomly sample 30 identities covering 2 hours as the validation set and leaving the remains as the training set.

To eliminate the potential training overlap and fairly evaluate the generative ability of each method, we sample 507 videos (around 74K frames in total) from TalkingHead-1KH [36] dataset, which comprises 170 identities and spans a wide range of languages. To conduct diverse tests, we formulate two test sets from the sampled 507 videos: a paired test set with the original video and speech, and an unpaired test with randomly sampled speech. By default, we conduct all the comparison experiments on the paired test set. We also provide comparisons with baseline methods in the unpaired test set.

Metric. We utilize various metrics including objective and subjective ones to provide an overall evaluation of our method.

- **Objective Metrics.** We adopt the objective metrics used in previous studies [6, 13, 18, 27, 32], including metrics to evaluate visual quality, lip sync accuracy and identity consistency. Specifically, we report commonly used PSNR, SSIM [40], LPIPS [43] and FID [19] to evaluate the generated visual quality. We adopt SyncNet [7] distance and conference scores, denoted as

Table 4: Comparisons of our appearance generation model with baseline. See Sec. 4.1 for details.

Method	PSNR \uparrow	SSIM \uparrow	LPIPS \downarrow	FID \downarrow
GAIA [18]	24.205	0.757	0.175	14.568
MyTalk (ours)	34.153	0.926	0.092	4.224

Table 5: Ablation study on condition types in motion generation model. Sec. 4.2 gives detailed explanation.

Method	Sync $_{dist}$ \downarrow	ID $_{sim}$ \uparrow
Ours (ID embed. cross-atten.)	6.544	0.947
concat. key landmark	6.718	0.923
add key landmark	7.509	0.932
key landmark cross-atten.	6.814	0.914

Sync $_{dist}$ and Sync $_{conf}$, to measure the lip sync quality. Inspired by [13], we leverage the ArcFace [9] network to compute the feature cosine similarity, denoted as ID $_{sim}$, between the ground truth and generated video frames, and use it to check the identity preservation ability.

- **Subjective Metrics.** We adopt four subjective metrics including visual quality, lip-sync quality, visual details preservation and identity consistency. In our user studies, we invite 20 participants to rate the talking videos generated by different methods. Participants are asked to rate a total of 44 videos on a 1-5 scale, with the average scores being reported.

Implementation Details. The identity extractor, motion generation model, and appearance generation model are trained separately. We adopt the Adam [22] optimizer for each model training. We perform all the experiments on 8 V100 GPUS. The identity extractor is trained for 100 epochs with a basic learning rate of $1e^{-6}$. The speech-driven motion generation model is trained for 3.5K epochs with an inverse square root learning rate schedule, and its basic learning rate is $1e^{-4}$. The appearance generation model is trained for 10 epochs on 256×256 resolution with a stable learning rate of $1e^{-6}$. The landmark sequence is padded to have a uniform length of 250 frames.

Results. We compare our proposed MyTalk with previous methods, including Wav2Lip [27], VideoReTalking [6] and TalkLip [35], with both objective (in Tab. 1 and Tab. 2) and subjective (in Tab. 3) evaluations. It can be observed that MyTalk surpasses all the baselines by a large margin in terms of visual quality and identity similarity, showcasing our great success in visual details preservation. Specifically, as shown in Fig. 2 (b), other methods tend to lose the original lip appearance or produce a blurred one, whereas our approach effectively preserves the lip details. Moreover, MyTalk consistently delivers superior lip-sync quality with both paired and unpaired test sets. However, comparing the lip-sync quality in Tab. 2, the performance of other methods all shows an obvious decline when handling the unpaired test set. Our leading results in Tab. 3 further demonstrate the effectiveness of MyTalk in visual details preservation and lip-sync quality. In addition, we compare our appearance generation model with the GAIA [18], and the results in Tab. 4 affirm our effectiveness in terms of visual quality.

Table 6: Ablation study of loss de-
sign in motion generation model. See
 Sec. 4.2 for details.

Method	Sync _{dist} ↓	ID _{sim} ↑
Ours (ID loss \times 1.0)	6.544	0.947
w/o ID loss	6.598	0.929
w. ID loss \times 2.0	7.010	0.951

Table 7: Ablation study on refer-
ence design in appearance genera-
tion model. See Sec. 4.2 for details.

Method	PSNR ↑	FID ↓
Ours (masked multi-ref.)	34.153	4.224
w. full single-ref.	31.750	6.62
w. masked single-ref.	32.759	6.453

4.2 Ablation Study

We conduct thorough ablation studies on the technical designs of our motion generation model and appearance generation model.

Condition Types in Motion Generation Model. Given that the model cannot successfully predict the entire facial landmarks conditioned solely on the upper face landmarks and speech input, we provide the model with the identity embedding of a reference frame for identity guidance. To demonstrate the validity of our reference information conditioning, we conduct a series of experiments on different condition types within our diffusion model. Specifically, we further explore three distinct conditioning strategies, including (1) concatenating the key landmark with input; (2) adding the key landmark feature to the input; and (3) integrating the key landmark via cross-attention.

In Tab. 5, our conditioning design outperforms others on both lip-sync quality and identity (ID) similarity. With other conditioning strategies, the model struggles to excel in both lip-sync quality and ID similarity, owing to the lack of constraint for identity learning. In contrast, our approach directly provides the model with identity features via our identity extractor.

Identity Loss in Motion Generation Model. To evaluate the effectiveness of our identity (ID) loss design, we further perform experiments using two different loss configurations: (1) excluding ID loss, and (2) incorporating ID loss with a weight of 2.0. As shown in Tab. 6, incorporating the ID loss significantly enhances the ID preservation. However, compared to MyTalk which uses the ID loss weight of 1.0, the higher ID loss weight compromises the model performance in lip sync.

Reference Design in Appearance Generation Model. We conducted experiments using three different reference configurations within our appearance generation model in Table 7. The first configuration uses a single image as the reference (full single-ref.). The second configuration employs a single image with non-lip region masked out (masked single-ref.). Finally, our MyTalk model implements a multi-reference setup that involves three masked reference images.

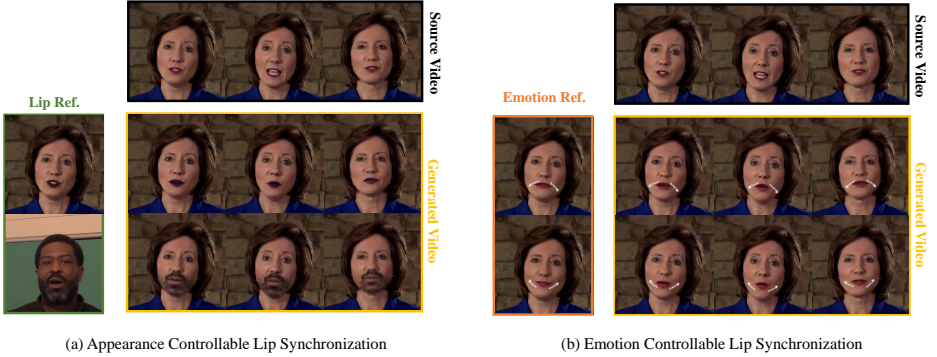


Fig. 4: Examples of controllable generation. Benefiting from our disentanglement and identity preservation designs, MyTalk shows novel properties in controlling appearance and emotion while editing the talking video.

The results in Table 7 indicate that masking operation helps in image quality and our multi-reference strategy further enhances the appearance generation.

4.3 Controllable Generation

Benefiting from our disentangled modeling, MyTalk can accurately integrate the appearance and motion conditions into generated videos as separate factors, which enables us to perform intriguing manipulations during the generation process. As shown in Fig. 4 (a), we can edit the lip region appearance by providing the model with a variety of reference images. In addition, we can emotionally control the talking video by using the emotion reference to guide both motion and appearance generation, see Fig. 4 (b) for visualization.

5 Conclusion

We propose to disentangle the motion and appearance in talking video lip sync and further divide the task into two sub-problems: speech-driven lip motion generation and visual appearance synthesis. We introduce MyTalk, a two-stage model, to separately generate the motion and appearance. Specifically, we utilize a speech-driven diffusion model to generate the motion, and propose an identity loss to preserve the identity. In the second stage, we introduce a motion-conditioned appearance generation model, which separately encodes the lip, non-lip appearance and motion, and then integrates them with a learned fusion module. Extensive experiments demonstrate the superiority of our method in visual detail preservation and lip-sync quality. Benefiting from the scaled training and disentangled modeling, MyTalk generalizes well to out-of-domain characters and shows great controllability to lip appearance and talking emotions. See the Appendix for more discussion on limitations and future work.

References

1. Blanz, V., Vetter, T.: A morphable model for the synthesis of 3d faces. *Seminal Graphics Papers: Pushing the Boundaries, Volume 2* (1999), <https://api.semanticscholar.org/CorpusID:203705211>
2. Blattmann, A., Dockhorn, T., Kulal, S., Mendelevitch, D., Kilian, M., Lorenz, D., Levi, Y., English, Z., Voleti, V., Letts, A., et al.: Stable video diffusion: Scaling latent video diffusion models to large datasets. *arXiv preprint arXiv:2311.15127* (2023)
3. Chen, H., Xia, M., He, Y., Zhang, Y., Cun, X., Yang, S., Xing, J., Liu, Y., Chen, Q., Wang, X., et al.: Videocrafter1: Open diffusion models for high-quality video generation. *arXiv preprint arXiv:2310.19512* (2023)
4. Chen, L., Cui, G., Kou, Z., Zheng, H., Xu, C.: What comprises a good talking-head video generation?: A survey and benchmark. *arXiv preprint arXiv:2005.03201* (2020)
5. Chen, L., Maddox, R.K., Duan, Z., Xu, C.: Hierarchical cross-modal talking face generation with dynamic pixel-wise loss. In: *Proceedings of the IEEE/CVF conference on computer vision and pattern recognition*. pp. 7832–7841 (2019)
6. Cheng, K., Cun, X., Zhang, Y., Xia, M., Yin, F., Zhu, M., Wang, X., Wang, J., Wang, N.: Videoretalking: Audio-based lip synchronization for talking head video editing in the wild. In: *SIGGRAPH Asia 2022 Conference Papers*. pp. 1–9 (2022)
7. Chung, J.S., Zisserman, A.: Out of time: automated lip sync in the wild. In: *Computer Vision–ACCV 2016 Workshops: ACCV 2016 International Workshops, Taipei, Taiwan, November 20–24, 2016, Revised Selected Papers, Part II* 13. pp. 251–263. Springer (2017)
8. Das, D., Biswas, S., Sinha, S., Bhowmick, B.: Speech-driven facial animation using cascaded gans for learning of motion and texture. In: *Computer Vision–ECCV 2020: 16th European Conference, Glasgow, UK, August 23–28, 2020, Proceedings, Part XXX* 16. pp. 408–424. Springer (2020)
9. Deng, J., Guo, J., Xue, N., Zafeiriou, S.: Arcface: Additive angular margin loss for deep face recognition. In: *Proceedings of the IEEE/CVF conference on computer vision and pattern recognition*. pp. 4690–4699 (2019)
10. Du, C., Chen, Q., He, T., Tan, X., Chen, X., Yu, K., Zhao, S., Bian, J.: Dae-talker: High fidelity speech-driven talking face generation with diffusion autoencoder. In: *Proceedings of the 31st ACM International Conference on Multimedia* (2023)
11. Esser, P., Rombach, R., Ommer, B.: Taming transformers for high-resolution image synthesis. In: *Proceedings of the IEEE/CVF conference on computer vision and pattern recognition*. pp. 12873–12883 (2021)
12. Gu, K., Zhou, Y., Huang, T.: Flnet: Landmark driven fetching and learning network for faithful talking facial animation synthesis. In: *Proceedings of the AAAI conference on artificial intelligence*. pp. 10861–10868 (2020)
13. Guan, J., Zhang, Z., Zhou, H., Hu, T., Wang, K., He, D., Feng, H., Liu, J., Ding, E., Liu, Z., et al.: Stylesync: High-fidelity generalized and personalized lip sync in style-based generator. In: *Proceedings of the IEEE/CVF Conference on Computer Vision and Pattern Recognition*. pp. 1505–1515 (2023)
14. Gulati, A., Qin, J., Chiu, C.C., Parmar, N., Zhang, Y., Yu, J., Han, W., Wang, S., Zhang, Z., Wu, Y., et al.: Conformer: Convolution-augmented transformer for speech recognition. *arXiv preprint arXiv:2005.08100* (2020)
15. Guo, Y., Chen, K., Liang, S., Liu, Y.J., Bao, H., Zhang, J.: Ad-nerf: Audio driven neural radiance fields for talking head synthesis. In: *Proceedings of the IEEE/CVF International Conference on Computer Vision (ICCV)*. pp. 5784–5794 (2021)

16. Guo, Y., Yang, C., Rao, A., Wang, Y., Qiao, Y., Lin, D., Dai, B.: Animatediff: Animate your personalized text-to-image diffusion models without specific tuning. arXiv preprint arXiv:2307.04725 (2023)
17. Hazirbas, C., Bitton, J., Dolhansky, B., Pan, J., Gordo, A., Ferrer, C.C.: Towards measuring fairness in ai: the casual conversations dataset. *IEEE Transactions on Biometrics, Behavior, and Identity Science* **4**(3), 324–332 (2021)
18. He, T., Guo, J., Yu, R., Wang, Y., Zhu, J., An, K., Li, L., Tan, X., Wang, C., Hu, H., et al.: Gaia: Zero-shot talking avatar generation. arXiv preprint arXiv:2311.15230 (2023)
19. Heusel, M., Ramsauer, H., Unterthiner, T., Nessler, B., Hochreiter, S.: Gans trained by a two time-scale update rule converge to a local nash equilibrium. *Advances in neural information processing systems* **30** (2017)
20. Ho, J., Jain, A., Abbeel, P.: Denoising diffusion probabilistic models. *Advances in neural information processing systems* **33**, 6840–6851 (2020)
21. Kazemi, V., Sullivan, J.: One millisecond face alignment with an ensemble of regression trees. In: *Proceedings of the IEEE conference on computer vision and pattern recognition*. pp. 1867–1874 (2014)
22. Kingma, D.P., Ba, J.: Adam: A method for stochastic optimization. arXiv preprint arXiv:1412.6980 (2014)
23. Kingma, D.P., Welling, M.: Auto-encoding variational bayes. In: *International Conference on Learning Representations (ICLR)* (2014)
24. Kondratyuk, D., Yu, L., Gu, X., Lezama, J., Huang, J., Hornung, R., Adam, H., Akbari, H., Alon, Y., Birodkar, V., et al.: Videopoet: A large language model for zero-shot video generation. arXiv preprint arXiv:2312.14125 (2023)
25. KR, P., Mukhopadhyay, R., Philip, J., Jha, A., Namboodiri, V., Jawahar, C.: Towards automatic face-to-face translation. In: *Proceedings of the 27th ACM international conference on multimedia*. pp. 1428–1436 (2019)
26. Porgali, B., Albiero, V., Ryda, J., Ferrer, C.C., Hazirbas, C.: The casual conversations v2 dataset. In: *Proceedings of the IEEE/CVF Conference on Computer Vision and Pattern Recognition*. pp. 10–17 (2023)
27. Prajwal, K., Mukhopadhyay, R., Namboodiri, V.P., Jawahar, C.: A lip sync expert is all you need for speech to lip generation in the wild. In: *Proceedings of the 28th ACM international conference on multimedia*. pp. 484–492 (2020)
28. Ren, Y., Li, G., Chen, Y., Li, T.H., Liu, S.: Pirenderer: Controllable portrait image generation via semantic neural rendering. In: *Proceedings of the IEEE/CVF International Conference on Computer Vision*. pp. 13759–13768 (2021)
29. Rombach, R., Blattmann, A., Lorenz, D., Esser, P., Ommer, B.: High-resolution image synthesis with latent diffusion models. In: *Proceedings of the IEEE/CVF conference on computer vision and pattern recognition*. pp. 10684–10695 (2022)
30. Schneider, S., Baevski, A., Collobert, R., Auli, M.: wav2vec: Unsupervised pre-training for speech recognition. arXiv preprint arXiv:1904.05862 (2019)
31. Shen, S., Li, W., Zhu, Z., Duan, Y., Zhou, J., Lu, J.: Learning dynamic facial radiance fields for few-shot talking head synthesis. In: *European Conference on Computer Vision*. pp. 666–682. Springer (2022)
32. Shen, S., Zhao, W., Meng, Z., Li, W., Zhu, Z., Zhou, J., Lu, J.: Difftalk: Crafting diffusion models for generalized talking head synthesis. arXiv preprint arXiv:2301.03786 (2023)
33. Tang, A., He, T., Tan, X., Ling, J., Li, R., Zhao, S., Song, L., Bian, J.: Memories are one-to-many mapping alleviators in talking face generation. arXiv preprint arXiv:2212.05005 (2022)

34. Thies, J., Elgharib, M., Tewari, A., Theobalt, C., Nießner, M.: Neural voice puppetry: Audio-driven facial reenactment. In: European Conference on Computer Vision (ECCV). pp. 716–731. Springer (2020)
35. Wang, J., Qian, X., Zhang, M., Tan, R.T., Li, H.: Seeing what you said: Talking face generation guided by a lip reading expert. In: Proceedings of the IEEE/CVF Conference on Computer Vision and Pattern Recognition. pp. 14653–14662 (2023)
36. Wang, T.C., Mallya, A., Liu, M.Y.: One-shot free-view neural talking-head synthesis for video conferencing. In: Proceedings of the IEEE/CVF conference on computer vision and pattern recognition. pp. 10039–10049 (2021)
37. Wang, Y., Yu, J., Yu, R., Zhang, J.: Unlimited-size diffusion restoration. In: Proceedings of the IEEE/CVF Conference on Computer Vision and Pattern Recognition. pp. 1160–1167 (2023)
38. Wang, Y., Yu, J., Zhang, J.: Zero-shot image restoration using denoising diffusion null-space model. arXiv preprint arXiv:2212.00490 (2022)
39. Wang, Y., Guo, J., Bai, J., Yu, R., He, T., Tan, X., Sun, X., Bian, J.: Instructavtar: Text-guided emotion and motion control for avatar generation. arXiv preprint arXiv:2405.15758 (2024)
40. Wang, Z., Bovik, A.C., Sheikh, H.R., Simoncelli, E.P.: Image quality assessment: from error visibility to structural similarity. *IEEE transactions on image processing* **13**(4), 600–612 (2004)
41. Wen, X., Wang, M., Richardt, C., Chen, Z.Y., Hu, S.M.: Photorealistic audio-driven video portraits. *IEEE Transactions on Visualization and Computer Graphics* **26**(12), 3457–3466 (2020)
42. Wood, E., Baltrušaitis, T., Hewitt, C., Dziadzio, S., Cashman, T.J., Shotton, J.: Fake it till you make it: face analysis in the wild using synthetic data alone. In: Proceedings of the IEEE/CVF International Conference on Computer Vision (ICCV). pp. 3681–3691 (2021)
43. Zhang, R., Isola, P., Efros, A.A., Shechtman, E., Wang, O.: The unreasonable effectiveness of deep features as a perceptual metric. In: Proceedings of the IEEE conference on computer vision and pattern recognition. pp. 586–595 (2018)
44. Zhang, W., Cun, X., Wang, X., Zhang, Y., Shen, X., Guo, Y., Shan, Y., Wang, F.: Sadtalker: Learning realistic 3d motion coefficients for stylized audio-driven single image talking face animation. In: Proceedings of the IEEE/CVF Conference on Computer Vision and Pattern Recognition. pp. 8652–8661 (2023)
45. Zhang, Z., Li, L., Ding, Y., Fan, C.: Flow-guided one-shot talking face generation with a high-resolution audio-visual dataset. In: Proceedings of the IEEE/CVF Conference on Computer Vision and Pattern Recognition. pp. 3661–3670 (2021)
46. Zhou, H., Sun, Y., Wu, W., Loy, C.C., Wang, X., Liu, Z.: Pose-controllable talking face generation by implicitly modularized audio-visual representation. In: Proceedings of the IEEE/CVF conference on computer vision and pattern recognition. pp. 4176–4186 (2021)
47. Zhou, Y., Han, X., Shechtman, E., Echevarria, J., Kalogerakis, E., Li, D.: Makeltalk: speaker-aware talking-head animation. *ACM Transactions On Graphics (TOG)* **39**(6), 1–15 (2020)

Appendix

We organize our supplementary material as follows:

- Sec. A gives qualitative comparisons with the baseline models mentioned in the main text.
- Sec. B provides some additional details on the workflow and architecture of the framework, its configuration, and dataset collection.
- Sec. C demonstrates the limitations and future work of our proposed MyTalk.

A Qualitative Comparison

We provide additional visualizations on qualitative comparisons to supplement the main paper. Fig. 5, Fig. 6 and Fig. 7 show the generation results on paired video-speech data, unpaired data from the same identity and unpaired data from different identities, respectively. The visualization comparisons all demonstrate our superiority in visual detail preservation and lip-sync quality.

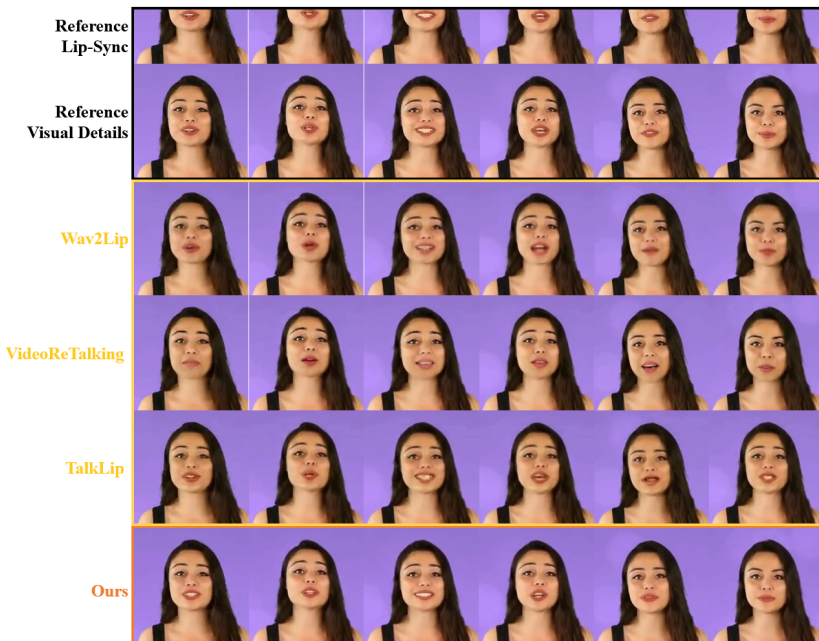


Fig. 5: Qualitative comparison on paired video-speech data.



Fig. 6: Qualitative comparison on unpaired video-speech data, wherein the video and speech are sampled from the same identity and different segments.

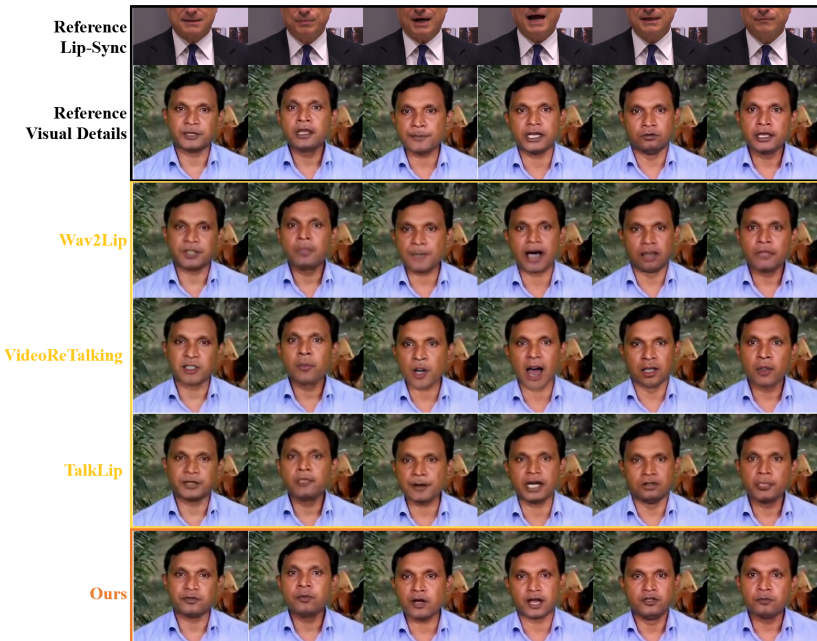


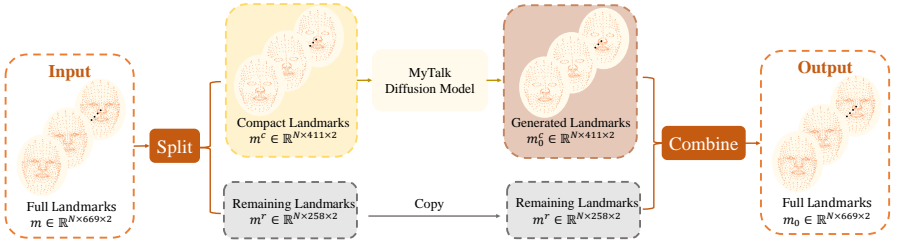
Fig. 7: Qualitative comparison on unpaired video-speech data, wherein the video and speech are sampled from different identities and segments.

B Additional Dataset and Framework Details

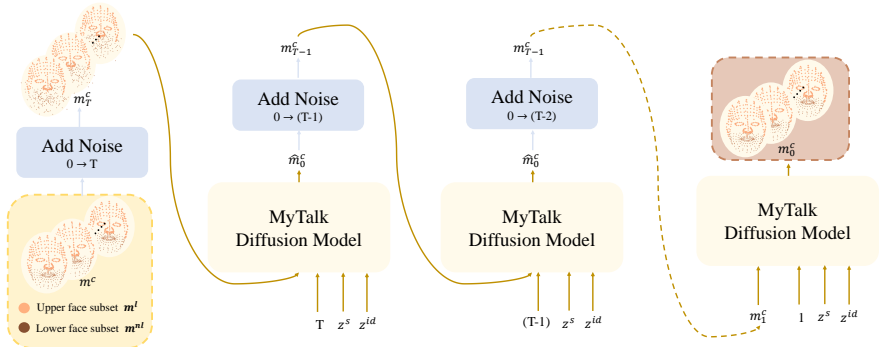
B.1 Framework Details

Speech-driven Motion Generation Model As demonstrated in Sec. 3.3 of the main text, we adopt a diffusion model to generate the landmark motion sequences. It takes the conditions $C = \{t, z^s, z^{id}\}$, where t is the diffusion time step, z^s is the speech feature, and z^{id} is the identity feature gotten by our identity extractor. The model design is shown in Fig. 3(a) of the main text, and the expanded details and the inference process are presented as follows.

As illustrated in Fig. 8 (a), we introduce some processes beyond the diffusion. Specifically, we divide the full landmarks $m \in \mathbb{R}^{N \times 669 \times 2}$ into two parts, the compact landmarks $m^c \in \mathbb{R}^{N \times 411 \times 2}$ and the remains $m^r \in \mathbb{R}^{N \times 258 \times 2}$. Here, the numbers 669, 411 and 258 represent the number of key points within each set of landmarks, with each point described by two-dimensional coordinates for its horizontal and vertical positions. This division is based on our empirical observations, which reveal that the remaining landmarks m^r contain unnecessary information for speech-related motion generation. Subsequently, as shown in Fig. 8 (b), the diffusion process is conducted on the compact landmark m^c . The generated landmarks m_0^c are then combined with the remaining landmarks m^r to form the final output m_0 .



(a) Illustration of pre-processing and post-processing steps in the motion generation stage



(b) Inference process of MyTalk's motion generation model

Fig. 8: Framework workflow of MyTalk's motion generation model.

Motion-conditioned Appearance Generation Model Our appearance generation model consists of three encoders, a FusionNet and one decoder, which is briefly illustrated in Fig. 3 (c). These encoders adopt the same architectures and the detailed architecture design is depicted in Fig. 9 (a). The symmetrical architecture of the decoder is shown in Fig. 9 (b). As illustrated in in Fig. 9 (c), we employ a FusionNet to fuse the lip and non-lip appearance features. This network takes the concatenated lip appearance feature and three non-lip appearance features as input and outputs the blended appearance feature.

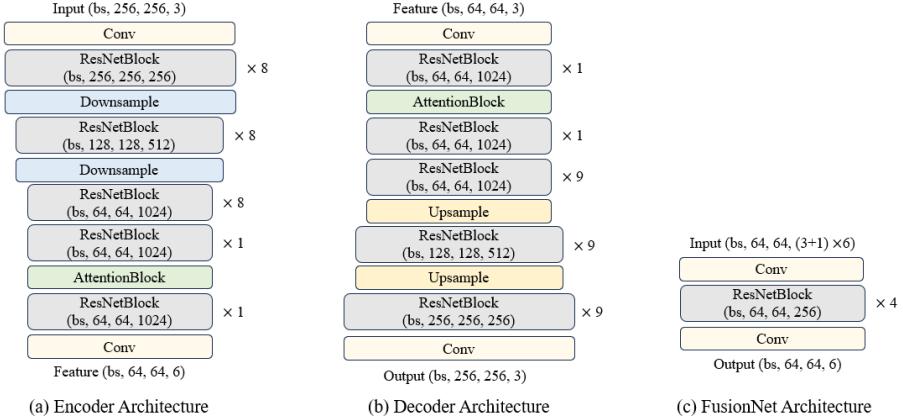


Fig. 9: Framework architecture of MyTalk’s appearance generation model.

Discussion on the Use of Landmark Like previous research [44], an alternative approach to motion generation is predicting the coefficients of a 3D Morphable Model (3DMM) [1]. However, we have observed in practice that it is challenging to obtain these coefficients for out-of-domain characters, especially when dealing with cartoon-based ones. To realize more generalized lip synchronization, we employ more effective and robust landmarks to represent the motion.

B.2 Dataset Details

As demonstrated in Sec. 4.1 of the main text, we assemble a large dataset comprising data from both public sources and internally collected datasets. Our appearance generation model is trained on the entire dataset, whereas our motion generation model adopts a subset of it. The high-quality subset excludes the parts with no speech, unaligned speech, and poor lip-syncing. The details are illustrated in Tab. 8.

B.3 Configuration

The model size and hyper-parameters of each component are detailed in Tab. 9.

Table 8: Statistics of our dataset.

Tasks	Time Duration	Number of Identity
Appear. Generation	1,169 hours	15,969
Motion Generation	148 hours	1,027

Table 9: Configuration of MyTalk.

Model	Component	Model Size	Hyper-parameters
Motion Generation Model	Audio Encoder	24.6M	Conformer Layers 4 Hidden Dim. 768 FFN Dim 2048 Attention Heads 8 Kernel Size 13 Dropout 0.1
	Audio Downsample	786K	Kernel Size 3 Stride 2 Padding 1
	Identity Extractor	4.3M	MLP Layers 4 Hidden Dim 768
	Conformer Backbone	188M	Conformer Layers 12 Hidden Dim. 768 FFN Dim 2048 Attention Heads 12 Kernel Size 5 Dropout 0.1
Appearance Generation Model	Lip Appear. Encoder Non-lip Appear. Encoder Landmark Encoder	237M	Hidden Dim. 256 ResnetBlock Layers 8 Kernel Size 3
	FusionNet	4.8M	Hidden Dim. 256 ResnetBlock Layers 4 Kernel Size 3
	Appear. Quant. Conv.	42	Kernel Size 1
	Landmark Quant. Conv.	42	
	Appear.-Landmark Quant. Conv.	21	
	Post-quant. Conv.	12	
	Decoder	280M	Hidden Dim. 256 ResnetBlock Layers 8 Kernel Size 3
	Discriminator	17.5M	KL Loss Weight $1.e^{-6}$ Dis. Loss Weight 0.5

C Limitations and Future Work

Firstly, as stated in Sec. B.2, the speech-to-motion generation training dataset is currently limited in size. We plan to expand this dataset to enhance the lip-sync quality and explore the scalability of our method. Secondly, as detailed in Table 10, our method requires more inference time due to the two-stage modeling. However, MyTalk outperforms other methods in terms of visual quality (PSNR, FID) and ID similarity (ID_{sim}) with a noticeable performance gap, which justifies extra time investment required by MyTalk. Finally, the current framework leverages a specific pre-trained landmark extractor [42], which may hinder the end-to-end learning of our model. We leave the effectiveness evaluation of our method on alternative types of landmarks (e.g., sparse landmark detected by [21]) and no landmarks (e.g., disentangle the motion and appearance without the help of landmarks) for future work.

Table 10: Comparisons with one-stage models.

Method	Metric Evaluation					Model Efficiency	
	PSNR \uparrow	FID \downarrow	ID_{sim} \uparrow	$Sync_{dist}$ \downarrow	$Sync_{conf}$ \uparrow	#param.(B)	Time(s)
Wav2Lip [27]	30.967	7.703	0.921	6.249	7.829	0.14	32.392
VideoReTalking [6]	29.628	9.628	0.895	6.978	6.986	0.69	897.671
TalkLip [35]	<u>31.140</u>	7.401	0.926	8.107	5.300	0.53	67.756
MyTalk(ours)	33.547	5.142	0.947	<u>6.544</u>	<u>7.461</u>	1.23	631.497